Energy 64 (2014) 771–778

Contents lists available at ScienceDirect

Energy

journal homepage: www.elsevier.com/locate/energy

Experimental investigation into gas/particle flow in a down-fired 350 MWe supercritical utility boiler at different over-fire air ratios

Chunlong Liu [a,b], Zhengqi Li [a,*], Xinjing Jing [a], Yiquan Xie [a], Qinghua Zhang [a], Qiudong Zong [a]

[a] School of Energy Science and Engineering, Harbin Institute of Technology, 92 West Dazhi Street, Harbin 150001, PR China
[b] Changchun Institute of Optics, Fine Mechanics and Physics, Chinese Academy of Sciences, Changchun 130033, China

ARTICLE INFO

Article history:
Received 4 June 2013
Received in revised form
3 November 2013
Accepted 7 November 2013
Available online 8 December 2013

Keywords:
Down-fired supercritical boiler
Gas/particle flow
Over-fire air ratio
Phase-Doppler anemometry

ABSTRACT

Gas/particle two-phase flow experiments at different over-fire air ratios were conducted using a 1:20 small-scale model of a down-fired 350 MWe superficial utility boiler designed with multiple injections and multiple staging combustion technology. The mean velocity, fluctuating velocity and particle volume flux were measured using particle dynamics anemometer measurements. None of four conditions of pulverized coal short-circuit occurred. When the over-fire air percentage was 1.9% and after the arch air flow reached the tertiary air, the position of maximum gas flow velocity of the arch secondary air and the maximum particle volume flux in the fuel-rich flow was close to and eroded the furnace hopper side wall. When the over-fire air percentage was increased to 9.6%, the position of maximum gas flow velocity of the arch secondary air and the maximum particle volume flux in the fuel-rich flow started to deviate from the hopper side wall but did not erode the furnace side wall. However, when the over-fire air percentage was 9.6%, the gas velocity of the arch air flow entering the furnace hopper was still high and the arch air flow downstream depth was too deep. Therefore, use of an over-fire air percentage greater than 19.1% was recommended.

Published by Elsevier Ltd.

1. Introduction

China is the largest anthracite producer and consumer with a forecasted increase in this trend as a result of economic development [1]. Anthracite, with a high degree of coalification and low volatile content is difficult to ignite and requires a long burnout time [2,3]. Because down-fired boilers have high furnace temperature and longer burnout time, they are suitable for burning anthracite and are used widely in China [4]. Most down-fired boilers generate fly ash of high carbon content and exhibit severe slagging, skew combustion and high NO_x emissions (>1300 mg/m^3 at 6% O_2) [5–8]. High NO_x emissions occur because unreasonable air velocity distributions cause pulverized coal in the lower part of the furnace to combust in an oxygen-rich state.

The control of NO_x emissions from down-fired boilers has become a topic of significance as promulgated legislation that commences on 1 July 2014 (thermal power plant air pollutant emission standards), has limited these emission concentrations to 200 mg/m^3 (at 6% O_2). Over-fire air (OFA) is an important means for reducing NO_x emissions, but few reports exist regarding FW (Foster Wheeler) and DBEL (Doosan Babcock Energy Limited) down-fired boilers in terms of OFA. Researchers have proposed installing OFA in FW boilers to reduce NO_x emissions [9]. Xue et al. [10] conducted experiments in a 0.9 MWe thermal test bench based on the prototype of a 300 MWe FW boiler to investigate pulverized coal combustion characteristics and NO_x emissions from the furnace after installation of OFA. Ren et al. and Li et al. [11–14] studied the influence of different OFA angles and OFA ratios on pulverized coal combustion characteristics and NO_x emissions from FW boilers by cold single-phase experiment and numerical simulation. Kuang et al. [15] studied the influence of OFA arrangement locations on aerodynamic fields and NO_x emissions in DBEL boilers by numerical simulation.

The study of gas/particle flow is significant for both the operation and transformation of large boilers, especially for pulverized coal combustion characteristics in the furnace. Compared with the pure gas phase, gas/particle flow characteristics are more complex and experimentation is the primary means to study gas/particle flow. Experiments have been conducted to investigate gas/particle flows in elbows and power plant boilers, Huber and Sommerfeld studied gas–solid flow behavior in pneumatic conveying systems by phase-Doppler anemometry [16]. Akilli et al. investigated gas–solid flow in a horizontal pipe after a 90 vertical-to-horizontal elbow by light probe [17,18]. Chen et al.

* Corresponding author. Tel.: +86 451 8641 8854; fax: +86 451 8641 2528.
E-mail address: green@hit.edu.cn (Z. Li).

0360-5442/$ – see front matter Published by Elsevier Ltd.
http://dx.doi.org/10.1016/j.energy.2013.11.025

studied gas/particle flow in a new swirl burner and the influence of different distance between Adjacent Rings the gas/particle flow in the centrally fuel rich burner [19,20]. Li et al. investigated gas/particle flow in different swirl burner structure and near the double swirl flow burner region in different outer secondary air vane angles [21,22]. Fan et al. studied gas/particle flow on a novel pulverized coal combustion technology for a large utility boiler by phase-Doppler anemometry [23]. Few experiments exist regarding the study of gas/particle flow in down-fired boilers: only Li et al. and Ren et al. have conducted gas/solid two-phase flow characterization experiments for a 300 MWe FW down-fired boiler [24,25] while Kuang et al. have performed experimental investigations for a 600 MWe MBEL down-fired boiler [26,27]. Limited literature is available on gas/particle flow experiments using different OFA rates in down-fired boilers. We have adopted multiple injections and multiple staging combustion technologies as proposed by Liu et al. [28] to design the combustion system of a down-fired 350 MWe boiler. OFA is installed in the upper furnace, as shown in Fig. 1. To investigate the influence of different OFA rates on particle behavior and flow characteristics in down-fired boilers, we constructed a 1:20 scale boiler cold two-phase model and performed measurements using a PDA (particle dynamics anemometer) system. Results from such experiments are beneficial in combustion system design and the operation of similar boilers.

2. Experimental setup

2.1. Utility boiler

Fig. 1 provides a structural diagram of the original down-fired 350 MWe boiler. Down-fired boilers are divided into an upper and lower furnace by the arch. The upper volume is smaller than the lower and the lower part of the furnace is the main combustion region. Twenty-four louver type bias burners are arranged on the front and rear arches and symmetrically to the furnace center. One group burner consists of two burners and there are six group burners on each arch. Each burner includes two primary, two vent, two inner, two outer and one oil air nozzle. Bias pulverized coal, arch secondary air and tertiary air are injected into the furnace through nozzles near the front and rear walls, through short nozzles and at a 25° angle through the down-dip device, respectively. Thirteen OFA nozzles were arranged symmetrically along the width of the furnace to its centerline on the front and rear wall of the upper furnace part. OFA was injected into the furnace at an angle and adopted the form of an inner straight and outer swirl flow.

2.2. Small-scale gas/particle flow experiments

The gas/solid two-phase cold-flow experimental system is illustrated in Fig. 2. It consists of an induced-draft fan, a small-scale furnace model, a power feeder, a cyclone separator and a three-dimensional PDA. In the test rig model, the measurement origin is the point of intersection between the central height of the primary air nozzle exit and front wall. For each measurement point, X_0 denotes the horizontal distance between the front and rear walls in the lower part of the furnace while X signifies the distance between the measurement point and origin in the horizontal direction.

Ten cross-sections were selected for the measurement process, namely $H/H_0 = 0.07$, 0.14, 0.21, 0.28, 0.35, 0.42, 0.437, 0.455, 0524 and 0.594 where H_0 is the vertical distance between the outlet of the fuel-rich flow nozzle and the upper edge of the dry bottom hopper, while H is the vertical distance from the measurement point to the outlet of the fuel-rich flow nozzle. Several measurement points were selected along each cross-section for data collection. The arrangement for the measurement points

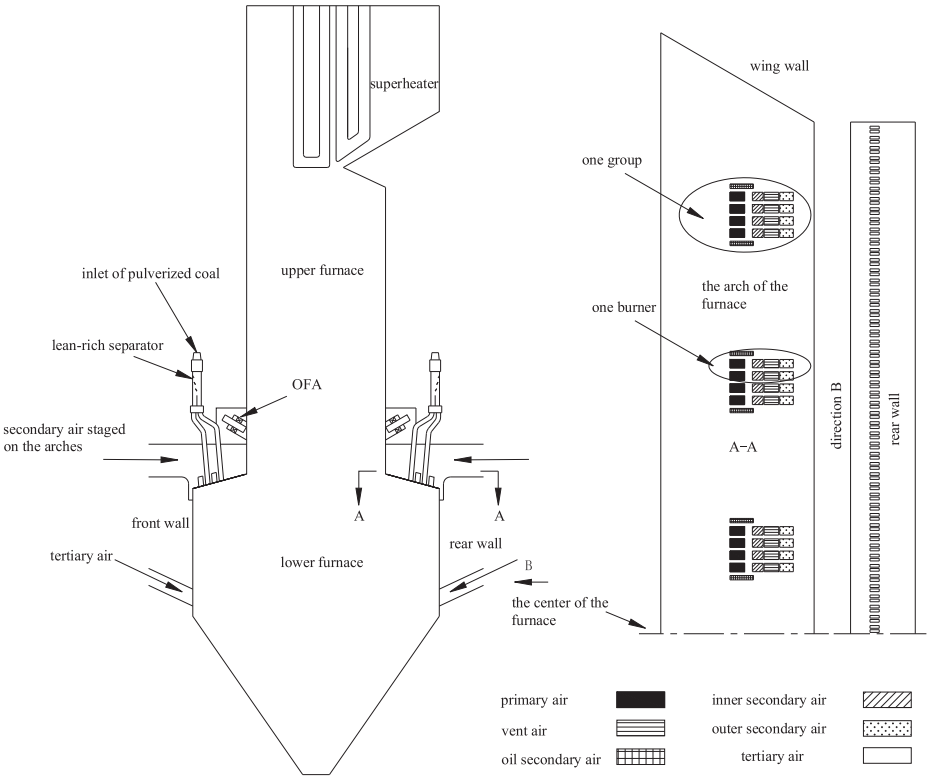

Fig. 1. Combustion system of down-fired 350 MWe boiler.

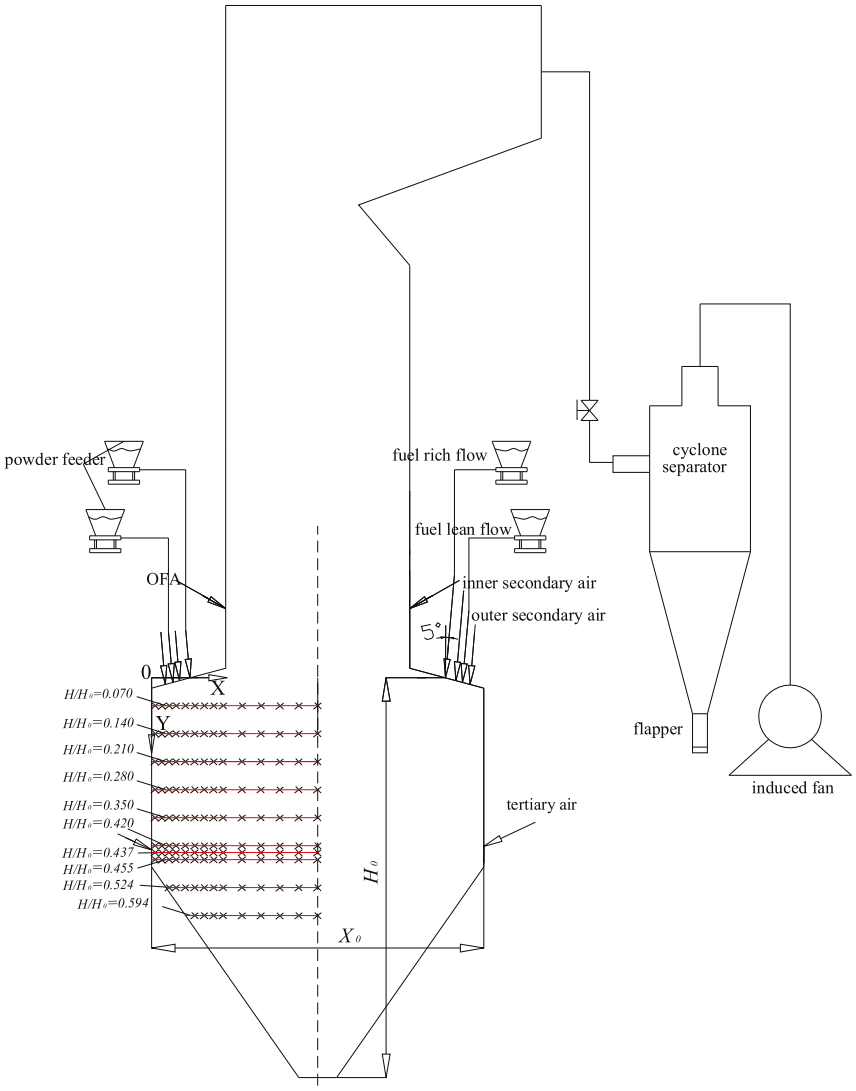

Fig. 2. Schematic of gas/solid two-phase cold-flow experimental system.

was relatively dense in the fuel-rich zone below the inner secondary, outer secondary, primary and vent air while measurement points in the fuel-lean zone were relatively sparse.

All the air flux into the model was measured using Venturi tube flow meters with a measurement error in air flow rate of less than 10%. Glass beads were fed into the primary and vent air by powder feeder and then brought into the test rig by the primary air.

There are several aspects to consider when building the test rig we used to conduct our cold two-phase experiments:

1. Geometric similarity: the ratio of model rig to full scale boiler is 1:20 and is therefore convenient for measurement using the PDA system.
2. Under the same conditions for the model and prototype, the ratio of momentum flux rate of model air flows should be consistent with the full-scale boiler.
3. Under the same conditions for the model and prototype, the Reynolds number of the primary and secondary air exits must be larger than 10,000 to ensure the air flows are self-modeling.
4. In gas/particle experiments, the coarse glass bead diameter is 48.15 μm while that of the fine glass beads is 14.35 μm. The furnace also has a certain amount of swirl and the Froude criterion is ignored in the present gas/particle flow experiments.

The gas/particle two-phase flow is considered to be similar to the flow conditions of the real furnace when the aforementioned criteria are met.

A three-dimensional model of PDA constructed by DANTEC Company was used in the gas/particle flow experiments. It consists of an argon laser, a transmitter, fiber optics, receiver optics, signal processors, a traversing system, a computer and a three-dimensional auto-coordinated rack. The velocity measurement range of the PDA system is 0–500 m/s with a measurement error of ±1%. The diameter measurement range was 0.5–1000 μm with a measurement error of ±4% and the particle concentration measurement range was $0–10^6$ particles/cm^3 with a measurement error of 15%. Detailed information and principles regarding PDA can be found in the literature [24–27,29].

During the experiments, particles 0–10 μm in size were used to represent gas-phase flow as they follow the air flow characteristics, while coarse particles 10–100 μm in size were used to represent solid-phase flow. Particle volume flow is measured by measuring particles from 0 to 100 μm. Four cases were arranged under conditions that the primary air and vent air are the design air flow and the total amount of over-the-arch secondary air, the tertiary air and the OFA is constant while the inclination of the tertiary 25° remains unchanged. The four OFA ratios were 1.9, 9.6, 19.1 and 28.7%. Table 1

documents the entrance velocities of the model rig under full load and some OFA parameters.

3. Results and discussion

V_x, V_y and V_{y0} denote the horizontal, vertical and exit velocities of the primary air nozzle in the vertical direction, respectively. The velocity positive direction is indicated by the arrows in Fig. 2. V_{max} is defined as the maximum velocity of each horizontal cross-section and would appear in the vertical cross-section for each over-the-arch nozzle. Meanwhile, the connecting line of V_{max}/V_{y0} of each horizontal cross-section is defined as the velocity decay curve.

3.1. Gas/particle two-phase velocity distribution

3.1.1. Gas/particle two-phase vertical velocity distribution

The vertical velocity distributions of the particle and gas phases in the furnace are depicted in Figs. 3 and 4. Both particle and gas phases follow a similar velocity distribution law. With the exception of the OFA ratio being 1.9%, under the other three OFA ratio conditions, the velocity in the center region of the furnace ($X/X_0 = 0.5$) is negative, namely two-phase flow in the center of the furnace is in an upward direction and the vertical velocity near the boundary walls of the furnace is positive. This means that the gas/particle two-phase flow is downward near the boundary walls. Therefore, a w-shaped flow field occurs.

From the cross-sections in Fig. 4 it can be seen that only one velocity peak appeared at $X/X_0 = 0.08$. The section corresponding to the inner secondary air nozzle and the corresponding velocity peak of the outer secondary air nozzle is undetectable. The reason may be that the particle concentration of the lean pulverized coal flow is small. The lean pulverized coal flow from the nozzle spreads around after being injected into the furnace because of the ejecting of secondary air and the PDA fails to detect the spread of lean particles in the pulverized coal air flow. The peak in the figure occurs mainly because of inner secondary air high speed injection into the furnace; the smaller the OFA ratio, the greater the vertical velocity peak value. When the OFA ratio decreases, the over-the-arch secondary air volume and velocity increase. The H/H_0 value increases gradually leading to gradual decreases in cross-section along the furnace height direction and peak speed. The main reason for this phenomenon is that the over-the-arch downward air flow in the downward process has diffused gradually and mixed with the surrounding gas. In the $H/H_0 = 0.455$ section, the peak value of the vertical velocity increases slightly, because the tertiary air nozzle faces downward at a 25° angle with the horizontal direction. Tertiary air has an ejection effect on over-the-arch downward air flow and continues downward. In the $H/H_0 = 0.594$ section, the peak value has been reduced, mainly because of diffusion after the over-the-arch downward air flow has mixed with tertiary air flow. With an OFA ratio of 1.9% in this section, the mostly vertical velocity is negative and the air flows upward. Because the horizontal velocity of the tertiary air is too high, the air flow momentum is still large after the front and rear wall air flows intersect. Under this OFA ratio, a skewed flow field forms in the furnace. The three other conditions have similar velocity distributions.

Table 1
Exit parameters of each air flow at different OFA ratios.

Case (%)	Modeled velocities (m/s)					
	Primary air (W_P)	Vent air (W_V)	Inner secondary air (W_1)	Outer secondary air (W_2)	Tertiary air (W_3)	OFA (W_0)
1.9	10	10	26.41	26.41	26.41	1.22
9.6	10	10	23.72	23.72	23.72	6.08
19.1	10	10	20.37	20.37	20.37	12.16
28.7	10	10	17.02	17.02	17.02	18.24

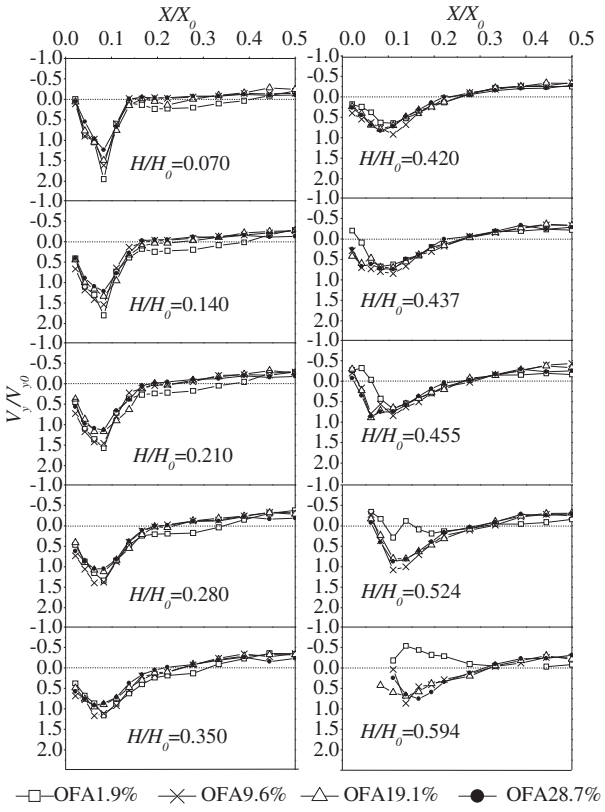

Fig. 3. Profiles of dimensionless vertical velocity distribution for air in furnace.

3.1.2. Analysis of gas/particle two-phase horizontal velocity distribution

Changes in OFA ratios have a small influence on the aerodynamic fields near the nozzles, but a large impact on the lower furnace aerodynamic fields. Furthermore, the smaller the OFA ratio, the greater the velocity in the center of furnace. From Figs. 5 and 6, the velocity distribution trend of the gas and solid phases is very similar. Before tertiary air injection into the furnace, the downward air flow velocity is relatively small, because the burner nozzle on the arch and the secondary air nozzle are injected separately into the furnace at a 5° vertical direction. Below the $H/H_0 = 0.437$ section, the injection of tertiary air forms an obvious peak and the mixing air flow horizontal momentum increases suddenly in each section. A maximum peak value appears in the section $H/H_0 = 0.455$, because the tertiary air nears the $H/H_0 = 0.437$ section and is injected down into the furnace at a horizontal direction of 25°. The section most affected by the tertiary air is below $H/H_0 = 0.437$. Below $H/H_0 = 0.280$, the OFA ratio of 1.9% is different from the other three and the horizontal velocity in the center furnace is still large.

It can be observed in Figs. 5 and 6 that when $H/H_0 = 0.07$ to 0.28, the horizontal velocity between the furnace center and primary air nozzles is mostly negative. Negative values indicate that the air flow direction is from the center of the furnace to the primary air pulverized coal flow and the regions of primary air pulverized coal flow and furnace center exist as a large recirculation zone. Hot gas recirculating can cause convective heat transfer with the ejected flow from the primary air nozzle and is beneficial to rapid primary

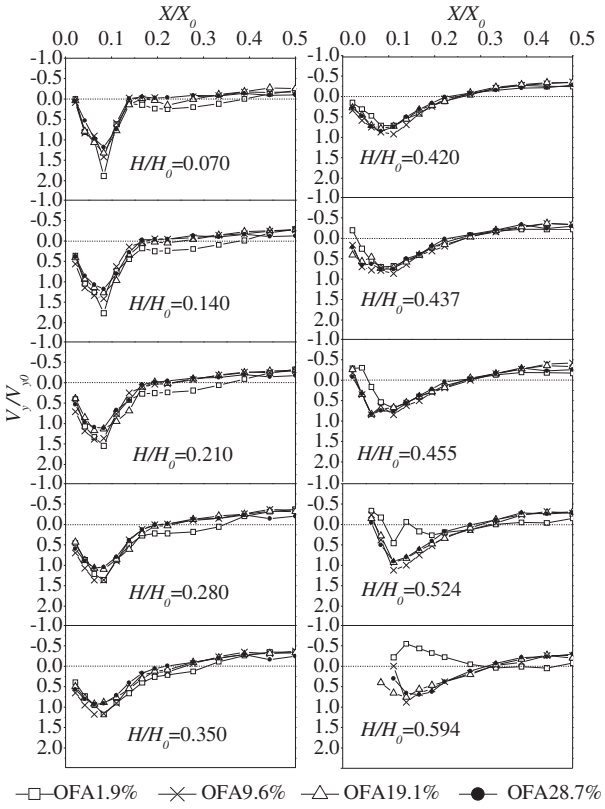

Fig. 4. Profiles of dimensionless vertical velocity distribution for particles in furnace.

air pulverized coal flow ignition and the combustion of pulverized coal. As the OFA ratio increases, the peak velocity decreases, recirculating less gas volume and reducing high temperature gas convective heat transfer.

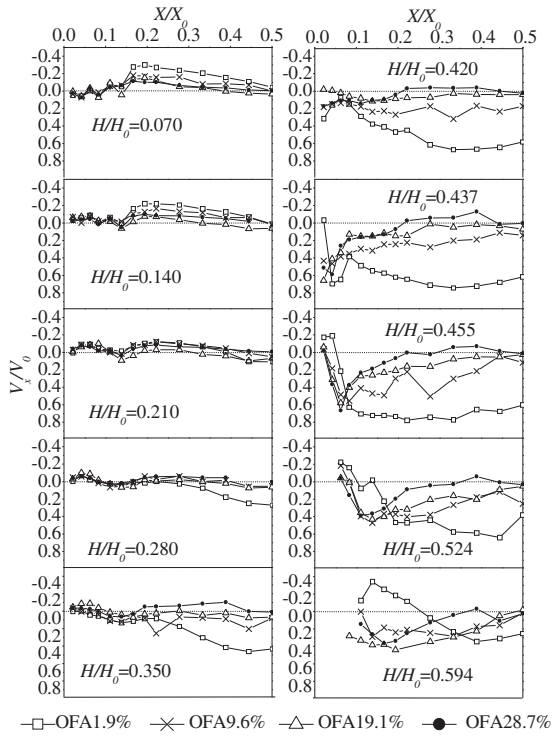

Fig. 5. Profiles of dimensionless horizontal velocity distribution for air in furnace.

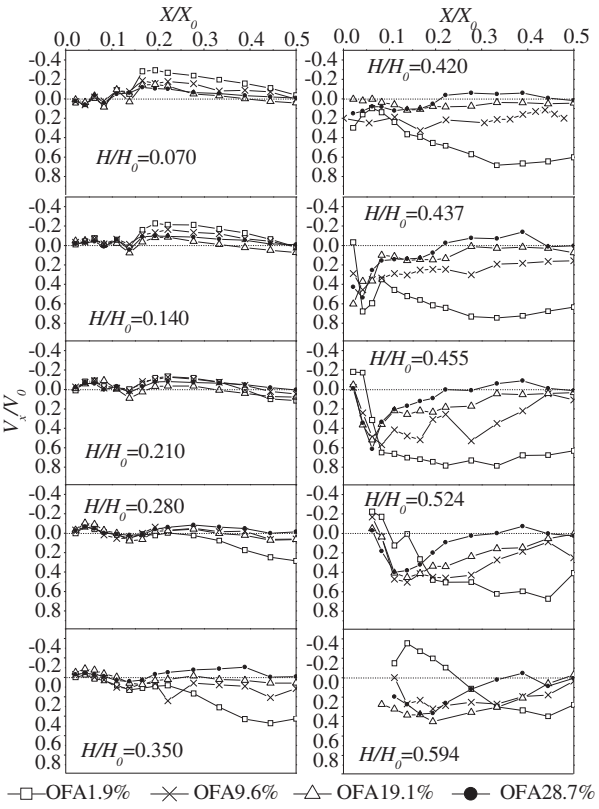

Fig. 6. Profiles of dimensionless horizontal velocity distribution for particles in furnace.

3.1.3. Distribution of velocity decay curves

Fig. 7 depicts the decay curves of the vertical maximum velocity of the gas-phase. In the furnace, the residence time of the pulverized coal is determined by its downward depth. For the boiler, as the residence time of the pulverized coal decreases, the pulverized coal combustion is insufficient. The released quantity of heat decreases and the flame center moves up, resulting in a decrease in furnace temperature and reduction in heat carried by the recirculation of flue gas. The high temperature gas is used for ignition and is conducive to combustion. We conclude from

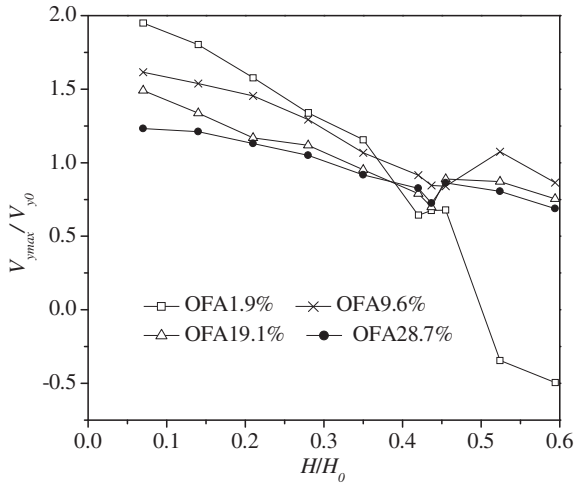

Fig. 7. Decay curves of air flow in the furnace at different OFA ratios.

Fig. 7 that the overall trend of maximum vertical velocity decreases continuously as the downward depth increases at $H/H_0 = 0.437$ and the injection of tertiary air increases the velocity slightly. When the OFA ratio is 9.6%, the injection effect was strongest and the increase in speed is also most significant. When OFA ratios are 19.1 and 28.7%, the increase in velocity is smaller, mainly because the velocity of the tertiary air decreases and the injection effect weakens as the OFA ratio increases. When the OFA ratio is 1.9%, the velocity is a large negative value for the same reasons as that given for Figs. 3 and 4. The flow field is deflected at the same time, causing uneven absorption of heat at the heating surface. The local high temperature in the furnace is likely to lead to slagging and this operating condition should be avoided in the actual operation of the boilers. When the OFA ratio is between 9.6 and 28.7%, the velocity distribution is much more reasonable, but when the ratio is 9.6%, the air flow velocity into the furnace hopper is large and may lead to the depth of the air flow above the arches decreasing excessively. When the OFA ratio is larger than 19.1%, the air flow velocity into the furnace hopper decreases and it is suggested that the OFA ratio be maintained above 19.1%.

3.2. Distribution of gas/particle two-phase fluctuation velocity

3.2.1. Distribution of gas/particle two-phase vertical fluctuation velocity

The profiles of the vertical fluctuation velocity distributions of gas and particles (Figs. 8 and 9) are similar. Every section between $H/H_0 = 0.07$ and 0.35 has two small peaks generated by inner and outer secondary air. After $H/H_0 = 0.35$, only one peak remains because the outer secondary air is attached to the wall and the left one is generated by the outer secondary air. After section $H/H_0 = 0.42$, the tertiary air mixes with the air flow from the arches. The confluence of the two air flows causes a large vertical fluctuation velocity and as the OFA ratio increases, the tertiary air volume is reduced gradually and the peak value of the vertical fluctuation velocity decreases.

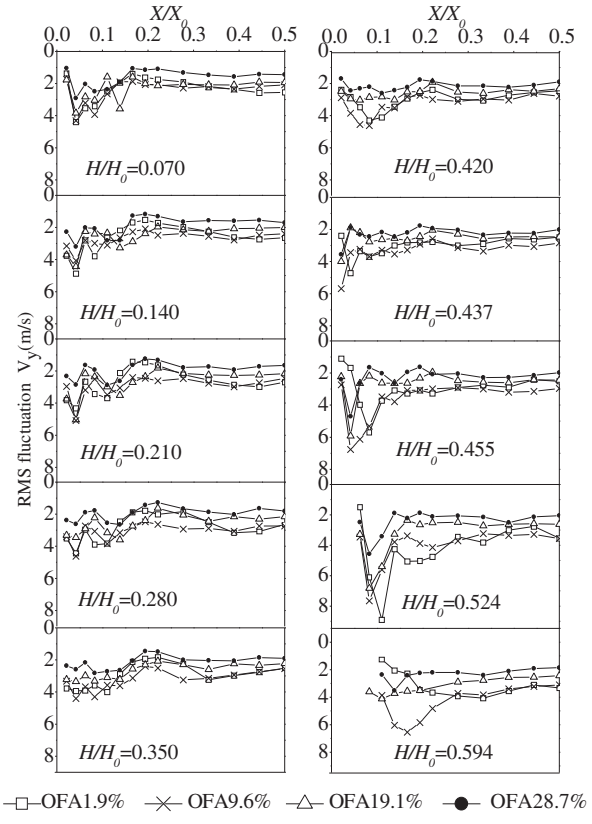

Fig. 8. Profiles of vertical rms fluctuation velocity distributions for air in furnace.

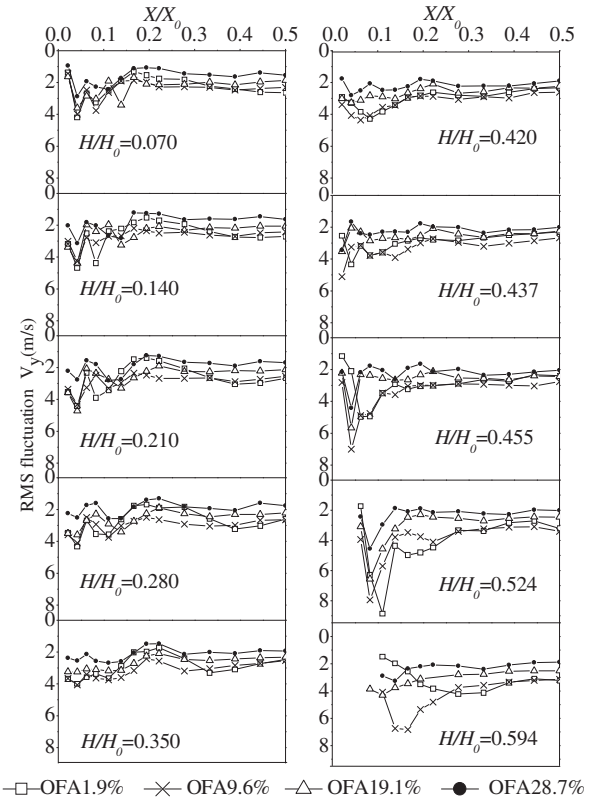

Fig. 9. Profiles of vertical rms fluctuation velocity distributions for particles in furnace.

3.2.2. Distribution of gas/particle two-phase horizontal fluctuation velocity

Figs. 10 and 11 are the profiles of the horizontal fluctuation velocity distributions of gas and particles and show that the pulsation curves are similar. As the horizontal velocity is small, the peak of the fluctuation velocity generated beneath the nozzle is not obvious. The fluctuation velocity in the furnace center is small between $H/H_0 = 0.07$ and 0.28. After $H/H_0 = 0.35$, the horizontal fluctuation velocity beneath this section increases gradually. After tertiary air injection into the furnace, in the entire area from the lower part of the vertical wall to the furnace hopper, the horizontal fluctuation velocity increases and indicates that the air flow mixes strongly here. When the OFA ratio increases, the horizontal velocity component of tertiary air reduces, mixing becomes weak with the air flow above the arches and the horizontal fluctuation velocity is also small.

3.3. Distribution of particle volume flux

The distribution of particle volume flux in Fig. 12 shows that the curve distribution trend is similar to the velocity distribution curve in the vertical direction. The particle volume flux has a relatively large maximum value after emission from the dense-phase nozzle. The apex position is below the dense-phase nozzle. There is no apex of particle volume flux for the lean-phase air flow since its particles enter the secondary air rapidly

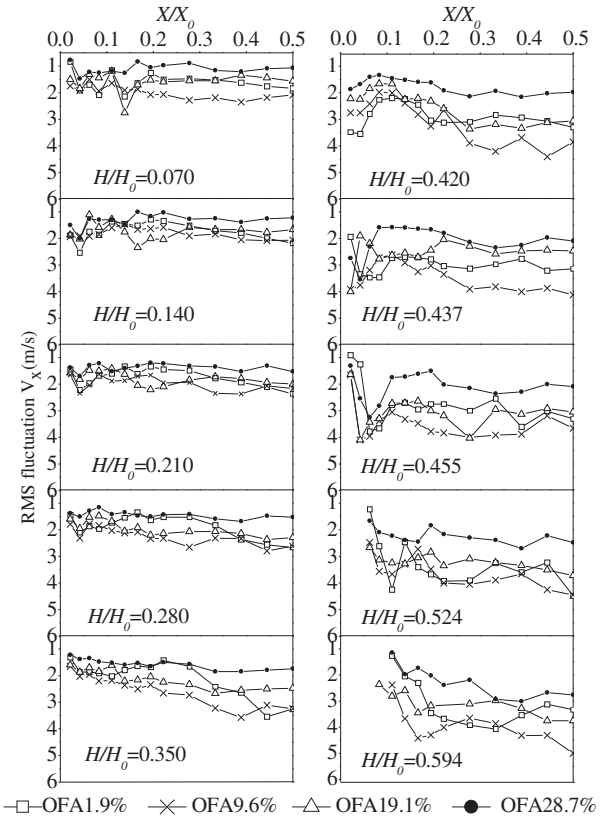

Fig. 10. Profiles of horizontal rms fluctuation velocity distributions for air in furnace.

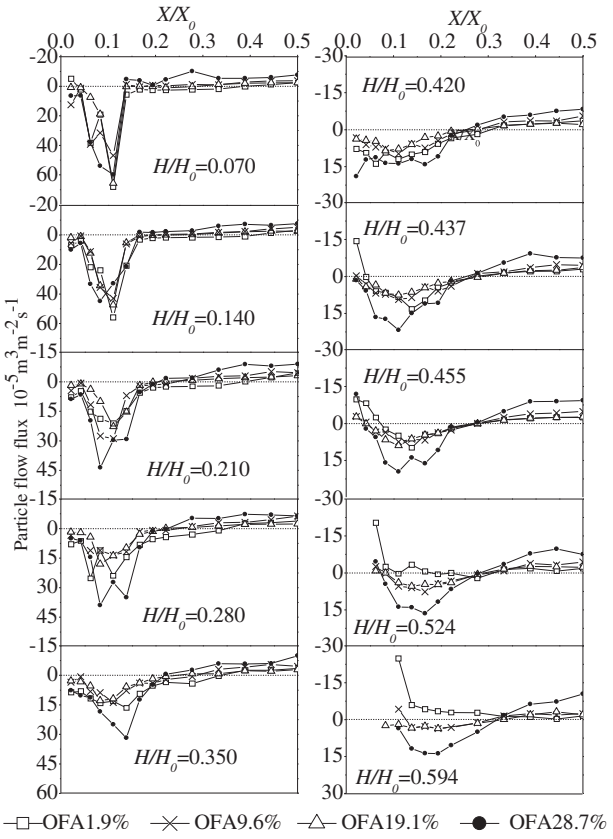

Fig. 12. Particle volume flux distributions in furnace.

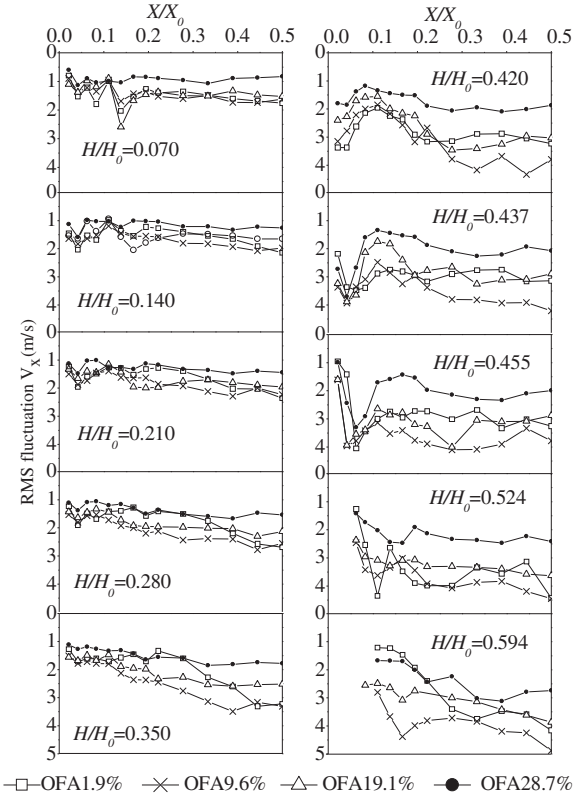

Fig. 11. Profiles of horizontal rms fluctuation velocity distributions for particles in furnace.

because of entrainment of the inner and outer secondary to force particles downward.

As the downward depth increases, the peak value of the particle volume flux declines and the particles disperse to the surrounding secondary air region quickly. The particle volume flux is relatively small in the furnace center region and mostly negative, indicating that particles travel upwards, following the air flow.

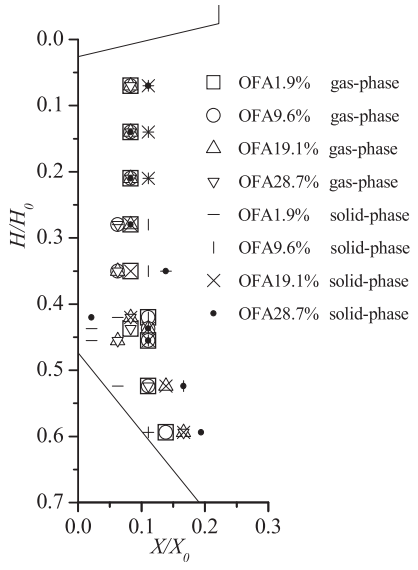

Fig. 13. Position of maximum air velocity and particle volume flux distribution at different OFA ratios.

3.4. Distribution of positions of maximum air velocity and particle volume flux

Fig. 13 depicts the distribution of positions of maximum air velocity and maximum particle volume flux at different OFA ratios. Over-the-arch secondary air and primary air both move downward next to the front wall before reaching the tertiary air and the principle among different OFA ratios is similar. After meeting the tertiary air, for a 1.9% OFA ratio, the maximum particle volume flux appears adjacent to the hopper side wall. The primary air brushes the hopper and causes slagging of the hopper and thermal fatigue. Unlike for an OFA ratio of 1.9%, the position of maximum air velocity and particle volume flux deviate from the side wall of the hopper under other OFA conditions. Meanwhile the air flow has a relatively large penetrating depth to avoid air flow short-circuiting.

4. Conclusions

This work reports on the use of a PDA system to investigate gas/particle flow characteristics for a down-fired 350 MWe supercritical utility boiler. The influence of OFA ratio on the aerodynamic field was also investigated. Experimental results will provide a reference for future work such as boiler design and its operation. Research into the four different OFA ratios, 1.9, 9.6, 19.1 and 28.7%, was conducted and the conclusions are as follows. For all four OFA ratios, the air flows reached the hopper area. However, for an OFA ratio of 1.9%, after meeting the tertiary air, the position of maximum gas velocity of the over-the-arch and maximum particle volume flux of the fuel-rich flow was close to the hopper side wall, brushing the hopper. As the OFA ratios increased, the positions of maximum gas velocity of the over-the-arch and the solid-phase maximum particle volume flux of the fuel-rich flow moved away from the hopper side wall. At an OFA ratio of 9.6%, the velocity of the over-the-arch air flow is still relatively large and may result in a large penetrating depth. Thus, use of an OFA ratio greater than 19.1% was recommended.

Acknowledgments

This work was supported by the Foundation for Innovative Research Groups of the National Natural Science Foundation of China (Grant No. 51121004).

References

[1] Gong XZ, Guo ZC, Wang Z. Variation on anthracite combustion efficiency with CeO_2 and Fe_2O_3 addition by differential thermal analysis (DTA). Energy 2010;35(2):506–11.
[2] Tan H, Niu Y, Wang X, Xu T, Hui S. Study of optimal pulverized coal concentration in a four-wall tangentially fired furnace. Appl Energy 2011;88(4):1164–8.
[3] Plumed A, Canadas L, Otero P, Espada M, Castro M, Gonzálcz J, et al. Primary measures for reduction of NOx in low volatile coals combustion. Coal Sci Technol 1995;24:1783–6.
[4] Fang QY, Wang HJ, Zhou HC, Lei L, Duan XL. Improving the performance of a 300 MW down-fired pulverized-coal utility boiler by inclining downward the F-layer secondary air. Energy Fuels 2010;24:4857–65.
[5] Kuang M, Li ZQ, Zhang Y, Chen XC, Jia JZ, Zhu QY. Asymmetric combustion characteristics and NOx emissions of a down-fired 300 MWe utility boiler at different boiler loads. Energy 2012;37(1):580–90.
[6] Li ZQ, Liu GK, Chen ZC, Zeng LY, Zhu QY. Effect of angle of arch-supplied overfire air on flow, combustion characteristics and NOx emissions of a down-fired utility boiler. Energy 2013;59:377–86.
[7] Ren F, Li ZQ, Liu GK, Chen ZC, Zhu QY. Combustion and NOx emissions characteristics of a down-fired 660-MWe utility boiler retrofitted with air-surrounding-fuel concept. Energy 2011;36(1):70–7.
[8] Burdett NA. The effects of air staging on NOx emissions from a 500 MW(e) down-fired boiler. J Inst Energy 1987;60:103–7.
[9] Leisse A, Lasthaus D. New experience gained from operating DS (swirl stage) burners. VGB Power Tech 2008;11:1–7.
[10] Xue S, Hui SE, Zhou Q, Xu T. Experimental study on NOx emission and unburnt carbon of a radial biased swirl burner for coal combustion. Energy Fuels 2009;23(7):3558–64.
[11] Ren F, Li ZQ, Chen ZC, Xu ZX, Yang GH. Influence of the over-fire air angle on the flow field in a down-fired furnace determined by a cold-flow experiment. Fuel 2011;90(3):997–1003.
[12] Ren F, Li ZQ, Liu GK, Chen ZC, Zhu QY. Numerical simulation of flow and combustion characteristics in a 300 MWe down-fired boiler with different overfire air angles. Energy Fuels 2011;25(4):1457–64.
[13] Li ZQ, Ren F, Chen ZC, Liu GK, Xu ZX. Improved NOx emissions and combustion characteristics for a retrofitted down-fired 300-MWe utility boiler. Environ Sci Technol 2010;44(10):3926–31.
[14] Li ZQ, Ren F, Chen ZC, Fan SB, Liu GK. Influence of the overfire air ratio on the NOx emission and combustion characteristics of a down-fired 300-MWe utility boiler. Environ Sci Technol 2010;44(16):6510–6.
[15] Kuang M, Li ZQ, Xu ST, Zhu XY, Zhang Y, Zhu QY. Impact of the overfire air location on combustion improvement and NOx abatement of a down-fired 350 MWe utility boiler with multiple injection and multiple staging. Energy Fuels 2011;25(10):4322–32.
[16] Huber N, Sommerfeld M. Characterization of the cross-sectional particle concentration distribution in pneumatic conveying systems. Powder Technol 1994;79(3):191–210.
[17] Akilli H, Levy E, Sahin B. Gas–solid flow behavior in a horizontal pipe after a 90° vertical-to-horizontal elbow. Powder Technol 2001;116(1):43–52.
[18] Akilli H, Levy EK, Sahin B. Investigation of gas-solid flow structure after a 90° vertical-to-horizontal elbow for low conveying gas velocities. Adv Powder Technol 2005;16(3):261–74.
[19] Chen ZC, Li ZQ, Zhu QY, Jing JP. Gas/particle flow and combustion characteristics and NOx emissions of a new swirl coal burner. Energy 2011;36(2):709–23.
[20] Chen ZC, Li ZQ, Wang ZW, Liu CL, Chen LZ, Zhu QY, et al. The influence of distance between adjacent rings on the gas/particle flow characteristics of conical rings concentrator. Energy 2011;36(5):2557–64.
[21] Zeng LY, Li ZQ, Zhao GB, Li J, Zhang FC, Shen SP, et al. The influence of swirl burner structure on the gas/particle flow characteristics. Energy 2011;36(10):6184–94.
[22] Jing JP, Li ZQ, Zhu QY, Chen ZC, Wang L, Chen LZ. Influence of the outer secondary air vane angle on the gas/particle flow characteristics near the double swirl flow burner region. Energy 2011;36(1):258–67.
[23] Fan WD, Li YY, Lin ZC, Zhang MC. PDA research on a novel pulverized coal combustion technology for a large utility boiler. Energy 2010;35(5):2141–8.
[24] Ren F, Li ZQ, Chen ZC, Wang J, Chen Z. Influence of the down-draft secondary air on the furnace aerodynamic characteristics of a down-fired boiler. Energy Fuels 2009;23(5):2437–43.
[25] Ren F, Li Z, Chen ZC, Xu ZX, Yang GH. Experimental investigations into gas/particle flows in a down-fired boiler: influence of the vent air ratio. Energy Fuels 2010;24(3):1592–602.
[26] Kuang M, Li Z, Zhu Q, Wang Y, Chen L, Zhang Y. Experimental gas/particle flow characteristics of a down-fired 600 MWe supercritical utility boiler at different staged-air ratios. Energy 2012;42(1):411–23.
[27] Kuang M, Li Z, Zhu Q, Zhang Y. Performance assessment of staged-air declination in improving asymmetric gas/particle flow characteristics within a down-fired 600 MWe supercritical utility boiler. Energy 2013;49:423–33.
[28] Liu CL, Li ZQ, Zhang X, Jing XJ, Zhang WZ, Chen ZC, et al. Aerodynamic characteristics within a cold small-scale model for a down-fired 350 MWe supercritical utility boiler at various primary air to vent air ratios. Energy 2012;47:294–301.
[29] Gillandt I, Fritsching U, Bauckhage K. Measurement of phase interaction in dispersed gas/particle two-phase flow. Int J Multiph Flow 2001;27(8):1313–32.

Glossary

X_0: horizontal distance between the front and rear walls in the lower part of the furnace (mm)
X: distance between the measurement point and origin in the horizontal direction (mm)
H_0: vertical distance between the outlet of the fuel-rich flow nozzle and the upper edge of the dry bottom hopper (mm)
H: vertical distance from the measurement point to the outlet of the fuel-rich flow nozzle (mm)
V_x: the horizontal velocity (m/s)
V_y: the vertical velocity (m/s)
V_{y0}: outlet velocity of the fuel-rich flow nozzle along the vertical direction (m/s)
V_{max}: maximum velocity of each horizontal cross-section and would appear in the vertical cross-section for each over-the-arch nozzle (m/s)
W: modeling velocities (m/s)

Subscripts

P: primary air
V: vent air
0: over-fire air
1: inner secondary air
2: outer secondary air
3: tertiary air